JOURNAL OF BACTERIOLOGY, Dec. 1997, p. 7759–7767 Vol. 179, No. 24
0021-9193/97/$04.00+0

Myxococcus xanthus sasS Encodes a Sensor Histidine Kinase Required for Early Developmental Gene Expression†

CHUN YANG AND HEIDI B. KAPLAN*

Department of Microbiology and Molecular Genetics, University of Texas Medical School at Houston, Houston, Texas 77030

Received 1 July 1997/Accepted 16 October 1997

Initiation of *Myxococcus xanthus* multicellular development requires integration of information concerning the cells' nutrient status and density. A gain-of-function mutation, *sasB7*, that bypasses both the starvation and high cell density requirements for developmental expression of the *4521* reporter gene, maps to the *sasS* gene. The wild-type *sasS* gene was cloned and sequenced. This gene is predicted to encode a sensor histidine protein kinase that appears to be a key element in the transduction of starvation and cell density inputs. The *sasS* null mutants express *4521* at a basal level, form defective fruiting bodies, and exhibit reduced sporulation efficiencies. These data indicate that the wild-type *sasS* gene product functions as a positive regulator of *4521* expression and participates in *M. xanthus* development. The N terminus of SasS is predicted to contain two transmembrane domains that would locate the protein to the cytoplasmic membrane. The *sasB7* mutation, an E139K missense mutation, maps to the predicted N-terminal periplasmic region. The C terminus of SasS contains all of the conserved residues typical of the sensor histidine protein kinases. SasS is predicted to be the sensor protein in a two-component system that integrates information required for *M. xanthus* developmental gene expression.

Multicellular development of *Myxococcus xanthus* is initiated by nutrient limitation and proceeds only if these gram-negative soil bacteria are at high density. More than 10^5 cells aggregate to form an organized mound, termed a fruiting body, inside of which the rod-shaped cells differentiate into environmentally resistant ovoid myxospores. This developmental program ensures the survival of the organism until nutrients are available and the spores can germinate (10, 11).

M. xanthus cells sense their nutrient status and density by using two different signals. Nutrient limitation is sensed, at least in part, by a rise in intracellular guanosine penta- and tetraphosphate ([p]ppGpp) levels (55). Cell density is sensed through A signal, a specific subset of amino acids at an extracellular concentration greater than 10 μM (36). The A signal is presumably generated when extracellular proteinases degrade the surface proteins of developing cells (35, 49). If the cells are at a density greater than about 3×10^8/ml, apparently the concentration of extracellular amino acids and peptides exceeds the critical A-signal threshold concentration (36). The transduction of the starvation and A signals and integration of this information within the first 1 to 2 h of development allow the cells to determine if conditions are appropriate to proceed through the early stages of fruiting body development (15, 26).

The expression of one class of genes expressed during early development requires independent input from both starvation and A signals (4, 25). The best characterized member of this class is the gene *4521*, whose expression is monitored by a Tn*5 lac* transcriptional fusion, Ω4521 (31). In wild-type cells 1 to 2 h after starvation at high density, which presumably allows the A-signal concentration to surpass its 10 μM threshold (36), *4521* expression is induced more than 10-fold over its basal level (25, 34, 50). In *asg* (A-signal-generating) mutants which cannot generate A signal, the expression of *4521* remains at its basal level even when the mutants are starved at high density (25, 34, 50). The *asg* genes map to three unlinked loci: *asgA*, *asgB*, and *asgC* (33). The DNA sequences of the *asg* genes indicate that they encode regulatory proteins required for A-signal production (8, 48, 50). The absence of any one of these regulators results in arrest at an early stage of development (17, 38). The expression of *4521* can be restored in the *asg* mutants by the addition of exogenous A signal or the presence of *asg* suppressor mutations, designated *sas.*

Studies of the *cis*-acting elements controlling *4521* expression revealed that the *4521* promoter is a member of the sigma54 family (29). Related studies have shown that a regulatory region of at least 146 bp upstream of the transcription start site is required for wild-type *4521* expression during growth and development (15). It is anticipated that, similarly to other sigma54-dependent promoters, an NtrC-like activator binding upstream of the transcription start site will be required for *4521* open complex formation (37, 43).

To identify the elements in the starvation and A-signal transduction pathways, second-site mutations that permit inappropriate *4521* gene expression were isolated in an *asgB480* background (25). Six suppressor mutants (*sasB5*, *-7*, *-14*, *-15*, *-16*, and *-17*) were isolated that bypass both the starvation and A-signal requirements for *4521* expression. In these mutants *4521* is expressed during growth and development in the absence of A signal (25). This study has focused on the *sasS* gene of the *sasB* locus that encodes a key regulator of *4521* expression. This gene, to which the *sasB7* mutation maps, is predicted to encode a classic transmembrane histidine protein kinase of the sensor protein family of the two-component signal transduction systems (21). SasS most likely functions by controlling the phosphorylation level of a downstream response regulator that regulates early developmental gene expression.

* Corresponding author. Mailing address: Department of Microbiology and Molecular Genetics, The University of Texas Medical School, 6431 Fannin, 1.765 JFB, Houston, TX 77030. Phone: (713) 500-5448. Fax: (713) 500-5499. E-mail: hkaplan@utmmg.med.uth.tmc.edu.

†This article is dedicated to Dale Kaiser in honor of his 70th birthday.

TABLE 1. Plasmid and strain list

Plasmid or strain	Relevant characteristics	Source, reference, or construction
Plasmids		
pBluescript SK$^+$	Amp^r	Stratagene
pBGS18	Kan^r	57
pHBK429	Kan^r	16
pYC274	Kan^r; Mx8 phage *attP* site	2.8-kb *Sma*I fragment of the *M. xanthus* Mx8 *attP* ligated with *Dra*I-digested pBGS18
pYC1001	Kan^r *sasB*$^+$	8-kb insert containing a portion of the *sasB* locus, resulting from in situ cloning of HK1403 chromosomal DNA
pYC1006	Kan^r *sasB*$^+$ *attP*	9.5-kb *Eco*RI-*Bgl*II fragment of pYC1001 ligated into *Eco*RI-*Bam*HI-digested pYC274
pYC1003	Kan^r; fragment of pYC1001	2.5-kb *Sac*I-*Xho*I fragment of pYC1001 ligated into *Sma*I-*Sal*I-digested pBGS18
pYC1004	Kan^r; fragment of pYC1001	1.1-kb *Sac*I fragment of pYC1001 ligated into pBGS18
pYC1018	Kan^r; fragment of pYC1001	1.8-kb *Sac*I fragment of pYC1001 ligated into pBGS18
pYC1020	Kan^r; fragment of pYC1001	2.7-kb *Sal*I-*Sph*I fragment of pYC1001 ligated into pBGS18
pYC1025	Kan^r *attP*; fragment of pYC1001	2.7-kb *Sal*I-*Sph*I fragment of pYC1001 ligated into pYC274
pYC1033	Kan^r; fragment of pYC1001	1.2-kb *Sma*I-*Sph*I fragment of pYC1001 ligated into pBGS18
pYC1101	Amp^r; fragment of pYC1001	700-bp *Sal*I-*Sac*I fragment of pYC1001 ligated into *Sma*I site of pBluescript SK$^+$
pYC1102	Amp^r; fragment of pYC1001	800-bp *Sac*I-*Sma*I fragment of pYC1001 ligated into *Sma*I site of pBluescript SK$^+$
pYC1104	Amp^r; fragment of pYC1001	2.0-kb *Sac*I-*Sph*I fragment of pYC1001 ligated into *Sma*I site of pBluescript SK$^+$
pYC1120–pYC1128	Amp^r; fragments of pYC1104	Exonuclease III-generated DNA fragments of pYC1104
pYC1202	Kan^r; 7.8-kb *Eco*RI-*Sph*I fragment of *sasB* locus from *sasB7* mutant DK6625	7.8-kb insert of the *sasB* locus resulting from in situ cloning of DK6625 chromosomal DNA containing the *sasB7* mutation
pYC1206	Amp^r; fragment of pYC1001 containing the *sasS* gene	4.5-kb *Sph*I fragment of pYC1001 ligated into the *Sma*I-digested pBluescript SK$^+$
pYC1207	Kan^r *sasS*::*kan*Ω	*kan*Ω cassette ligated into the *Nru*I-digested pYC1206
pYC1209	Kan^r; internal fragment of *sasS* gene	1.2-kb *Nru*I-*Sma*I of pYC1020 ligated into *Sma*I-digested pBGS18
pYC1215	Kan^r *sasS*::*lacZ*	Promoterless *lacZ* ligated to the *Sac*I site of *sasS*
pYC1220	Kan^r; fragment of pYC1202	850-bp *Sal*I-*Pst*I fragment of pYC1202 ligated into pBGS18
E. coli DH5α	*supE44* Δ*lacU169* (ϕ80 *lacZ* ΔM15 *hsdR17 recA1 endA1 gyrA96 thi-1 relA1*)	18
M. xanthus		
DK101	*sglA1*	22
DK480	*sglA1 asg480*	17
DK1622	Wild type	24
DK6600	Tn*5 lac* Ω4521(Tc^r) *sglA1 asgB480*	25
DK6620	Tn*5 lac* Ω4521(Tc^r) *sglA1*	25
DK6625	Tn*5 lac* Ω4521(Tc^r) *sglA1 asgB480 sasB7*	25
DK6661	Tn*5* Ω6658 *sglA1 sasB7*	H. Kaplan from DK6659 (25)
DK6662	Tn*5* Ω6658 (Tc^r) *sglA1*	H. Kaplan from DK6660 (25)
HK1403	Tn*5* Ω6658 (Tc^r)::pHBK429 *sglA1*	Introduction of pHBK429 into DK6662 by electroporation
HK1407	Tn*5 lac* Ω4521(Tc^r) *sglA1 asgB480 sasB7*	Introduction of pYC1033 into DK6625 by electroporation
HK1412	Tn*5 lac* Ω4521(Tc^r) *sglA1 sasB7* Tn*5* Ω6658	Generalized Mx4 transduction from donor strain DK6661 to recipient strain DK6620
HK1501	Tn*5 lac* Ω4521(Tc^r) *sglA1 sasS*::*kan*Ω	Introduction of linearized pYC1207 into DK6620 by electroporation
HK1502	Kan^r *sglA1 asgB480 sasS* disrupted by an internal fragment	Introduction of pYC1209 into DK480 by electroporation
HK1503	Kan^r *sglA1* Tn*5 lac* Ω4521(Tc^r) *sasS* disrupted by an internal fragment	Generalized Mx4 transduction from donor strain HK1502 to recipient strain DK6620
HK1504	*sasS*::*kan*Ω	Generalized Mx4 phage transduction from donor strain HK1501 to recipient strain DK1622
HK1509	*sasS*::*lacZ sglA1 asg480*	Introduction of pYC1215 into DK480 by electroporation
HK1510	*sasS*::*lacZ sglA1*	Generalized Mx4 transduction from donor strain HK1509 to recipient strain DK101

MATERIALS AND METHODS

Bacterial strains, plasmids, phages, and growth conditions. The plasmids and strains used in this study are listed in Table 1. Strains containing the Ω4521 Tn*5 lac* (Tc^r) insertion (31) allow the expression of the *4521* reporter gene to be monitored. Strain DK1622 is used as the wild type in tests of fruiting body formation and sporulation efficiency. Strain DK6625 carries *asgB480* and one *asgB480* suppressor mutation, *sasB7*, which restores *4521* expression (25). The myxophage Mx4 (*ts18 ts27 hrm*) (7, 12) is the temperature-sensitive, inducible phage used for generalized transduction of *M. xanthus* strains.

M. xanthus strains were grown with vigorous shaking at 32°C in CTT liquid medium (1% Casitone [Difco], 10 mM Tris-HCl [pH 7.6], 1 mM K_2HPO_4-KH_2PO_4 [pH 7.7], 8 mM $MgSO_4$; final pH of the mixture, 7.6) or on CTT agar (CTT liquid with 1.5% Bacto-Agar). Kanamycin at 40 μg/ml was added when appropriate. The growing cells were used in the mid-exponential phase (80 to 160 Klett units, which is approximately 4×10^8 to 8×10^8 cells per ml). *Escherichia coli* strains were grown in Luria-Bertani (LB) liquid medium (53) or on LB agar (LB liquid with 1.5% Bacto-Agar) which contained 100 μg of ampicillin/ml or 50 μg of kanamycin/ml when appropriate to maintain plasmids.

***M. xanthus* development and measurement of β-galactosidase specific activity and sporulation efficiency.** *M. xanthus* cells developed on TPM starvation agar (10 mM Tris-HCl [pH 7.6], 1 mM K_2HPO_4-KH_2PO_4 [pH 7.7], 8 mM $MgSO_4$, 1.5% Bacto-Agar) according to the method of Kroos et al. (31) were used for the measurement of developmental β-galactosidase specific activity. For development on starvation agar, growing cells in mid-exponential phase were harvested by centrifugation and the cell pellet was resuspended in TPM buffer at a density of 5×10^9 cells/ml. Drops of the cell suspension on dry TPM agar plates were incubated at 32°C, and at the appropriate times the cells were scraped from the agar, suspended in TPM buffer, and stored immediately at −20°C. The β-galactosidase specific activity of the thawed samples was quantitated by the method of Kroos et al. (31) as modified by Gulati et al. (15). Protein concentrations were determined by the Bradford assay (6), using a Bio-Rad reagent and immunoglobulin G as the protein standard.

M. xanthus cells developed in submerged culture, according to the protocol of Kuner and Kaiser (32) as modified by Kuspa et al. (34), were used for sporulation analysis. For development in submerged culture, mid-exponential phase *M. xanthus* cells were harvested, resuspended in MC7 buffer (10 mM morpholinepropanesulfonic acid [MOPS; pH 7.0], 1 mM $CaCl_2$) to a calculated density of 2.5×10^8/ml, and placed in 24-well tissue culture plates. The plates were incubated in a humid chamber at 32°C for 4 to 7 days. Under these conditions, the wild-type cells settle to form a thin mat on the bottom of the well and develop with timing similar to that seen on TPM agar. Fruiting bodies were observed under a dissecting microscope after 3 to 10 days of development.

The production of heat-resistant and sonication-resistant spores was measured in submerged culture preparations. Briefly, the cells were diluted to 10^8/ml with MC7 buffer and the plates were incubated for 2.5 h at 50°C. The suspensions were then sonicated to break the rod-shaped cells, and 10-fold dilutions were plated onto CTT nutrient agar. The number of viable spores was measured by counting the number of CFU.

Plasmid construction. The plasmid pYC1001 was directly cloned from the wild-type *M. xanthus* chromosome by the in situ cloning method described in Results. The other plasmids were constructed as described in Table 1. For mapping the *sasB7* mutation, plasmids pYC1003, pYC1004, pYC1018, and pYC1020 were constructed by using the vector pBGS18 (57) and plasmids pYC1006 and pYC1025 were constructed by using pYC274 (Table 1). For DNA sequencing analysis, all the DNA fragments were cloned into the vector pBluescript SK^+ (Stratagene). The DNA fragments present in plasmids pYC1101, pYC1102, and pYC1104 were subcloned from pYC1001. The DNA fragments present in pYC1120 through pYC1128 were generated by exonuclease III (Erase-A-Base system kit; Promega) digestion of pYC1104. For construction of the *sasS* insertional null mutation, the omega kanamycin cassette, which blocks transcription and translation in both directions (51), was used.

The protocols used, such as plasmid isolation, restriction endonuclease digestion, ligation in low-melting-point agarose, and other standard molecular biological techniques, are described by Sambrook et al. (53).

DNA sequence determination and computer analysis. The sequences of the *M. xanthus* DNA in plasmids pYC1101, pYC1102, pYC1104, and pYC1120 through pYC1128 were determined. The plasmids were purified with the QIAprep spin kit (Qiagen). The sequences of both strands of the 2.7-kb *Sal*I-*Sph*I region were determined at the DNA Core Facility of the Department of Microbiology and Molecular Genetics, University of Texas—Houston Medical School, with 373A and 373 prism DNA sequencers (Perkin-Elmer, Applied Biosystems Division) with *Taq* polymerase in a thermal cycling reaction. Both T7 and T3 primers were used.

The DNA sequences were aligned and edited with the SeqEd 675 DNA sequence editor program (Perkin-Elmer, Applied Biosystems Division). The University of Wisconsin Genetics Computer Group's sequence software package version 8.0 (9) was used for sequence analysis. The Codonpreference program predicted the open reading frames (ORFs) based on the G-C codon bias of the third position (2) in this high-G+C-content (67.5 mol%) organism (41). Searches were performed at the National Center for Biotechnology Information with the BLAST network service (1). The Pileup program aligned the protein sequences, the Bestfit program determined pairwise identities, the Motifs program was used to identify motifs in SasS, the Peptidestructure program was used to predict the secondary structure of SasS, the Pepplot program was used to predict the hydrophobicity of the protein, and the putative transmembrane domain of SasS was determined by TMpred program (http://www.science.adelaide.edu.au/microb./micro3/tmpred.htm).

Cloning of the *sasB7* allele and identification of the *sasB7* mutation. Mapping data indicated that the *sasB7* allele was close to the unique *Sac*I site in SasS. To determine the DNA alteration causing the *sasB7* mutation, the *sasS* region was cloned from the *sasB7* mutant strain DK6625, using a modification of the in situ cloning method of Gill et al. (13). In this case, the vector DNA which supplies the origin of replication and restriction sites for cloning adjacent DNA was targeted to integrate into the region adjacent to the *Sac*I site because it carried this adjacent region. Thus, to clone the *sasB7* allele, the 1.2-kb *Sma*I-*Sph*I fragment from pYC1120 cloned in the vector pBGS18 was introduced into DK6625. DNA was prepared from this strain (HK1407), digested with the *Eco*RI restriction enzyme, ligated, and used to transform *E. coli*, and plasmid pYC1202 was isolated. The *sasB7* allele was predicted to be contained within the 850-bp *Sal*I-*Pst*I region of pYC1202. This region was subcloned into pBGS18, yielding plasmid pYC1220. The DNA sequence of the complete *Sal*I-*Pst*I 850-bp insert was determined by automated sequencing.

DNA transfer methods. DNA was transferred from *E. coli* to *M. xanthus* by electroporation (27). DNA was transferred between *M. xanthus* strains by generalized transduction with myxophage Mx4 (12).

Amino acid rescue of *4521* expression at low cell densities. Phenotypic rescue of *4521* expression at low cell density was performed according to the method developed by Kuspa et al. (36). All of the strains used in this assay carry the social motility mutation *sglA1*, which causes a defect in cell-cell cohesion that allows the cells to remain in suspension. *M. xanthus* cells were harvested from mid-exponential stage and resuspended in 0.4 ml of MC7 buffer at a density of 1.25×10^8/ml in 24-well tissue culture plates. The A-signal amino acid proline was added to each well to generate final concentrations of 10 μM to 2 mM. The cell suspensions were incubated in a humid chamber at 32°C for 20 h and frozen immediately at −20°C. The β-galactosidase activities of the thawed samples were analyzed and normalized to cell number.

Nucleotide sequence accession number. The nucleotide sequence of *sasS* and its surrounding region has been assigned GenBank accession no. AF029787.

RESULTS

Cloning of the wild-type region corresponding to the *sasB7* mutation. The wild-type region corresponding to the *sasB7* mutation was cloned from the *M. xanthus* chromosome, using the in situ cloning method developed by R. Gill et al. (13). First, using Southern blot analysis, we obtained a restriction map of the *sasB* locus from the $SasB^+$ strain DK6662, containing Tn*5* Ω6658 linked to the wild-type version of the *sasB7* allele. *Eco*RI sites flanking Tn*5* Ω6658 were mapped at 8 and 22 kb on either side of the transposon (Fig. 1A). These *Eco*RI fragments were cloned by allowing the pHBK429 vector (16) to integrate into the chromosome at Tn*5* Ω6658, providing an *E. coli* origin of replication and restriction sites (including an *Eco*RI site) for cloning the adjacent DNA. The resulting strains, HK1403 and HK1406, each contain pHBK429 integrated in a different orientation. DNA from each strain was isolated, digested with *Eco*RI restriction enzyme, and ligated at low concentration to promote intramolecular ligations. Plasmid pYC1001 was purified from an *E. coli* colony transformed with HK1403-ligated DNA.

The 8-kb *M. xanthus* chromosomal DNA fragment carried on pYC1001 contains the wild-type version of the *sasB7* allele. This fragment restores the wild-type phenotype to the *sasB7* mutant DK6625 when it is present as a tandem duplication in the chromosome (Fig. 1B). The phenotype was determined by overlaying the transformants containing Ω4521 Tn*5* *lac* as a reporter of starvation- and A-signal-dependent gene expression with 0.04% 5-bromo-4-chloro-3-indolyl-β-D-galactopyranoside (X-Gal), the chromogenic substrate of β-galactosidase. Ninety percent of the selected transformants were $SasB^+$ (tan colonies when overlaid with X-Gal, identical to the *asgB480* parent), and 10% of the selected transformants were $SasB^-$ (blue colonies when overlaid with X-Gal). This restoration of the $SasB^+$ phenotype at 90% suggests that the fragment contains the complete wild-type transcription unit. In tandem duplications restoration of the wild-type phenotype at less than 100% is typical and is most likely a result of apparent gene conversion (58). Gene conversion in *M. xanthus* is documented to commonly occur at 10 to 25% in these types of crosses (16, 54, 58).

To ensure that the 8-kb fragment contained a complete transcription unit, it was integrated at the myxophage Mx8 attachment site, *attB*, and tested for its ability to restore the $SasB^+$ phenotype to DK6625. In this case, any cloned fragment that can restore the $SasB^+$ phenotype from this *trans* location must contain a complete transcription unit. Restoration at 100% would be expected because gene conversion should not occur in this type of cross. One hundred percent (3,000 of 3,000) of the selected transformants were $SasB^+$. These data

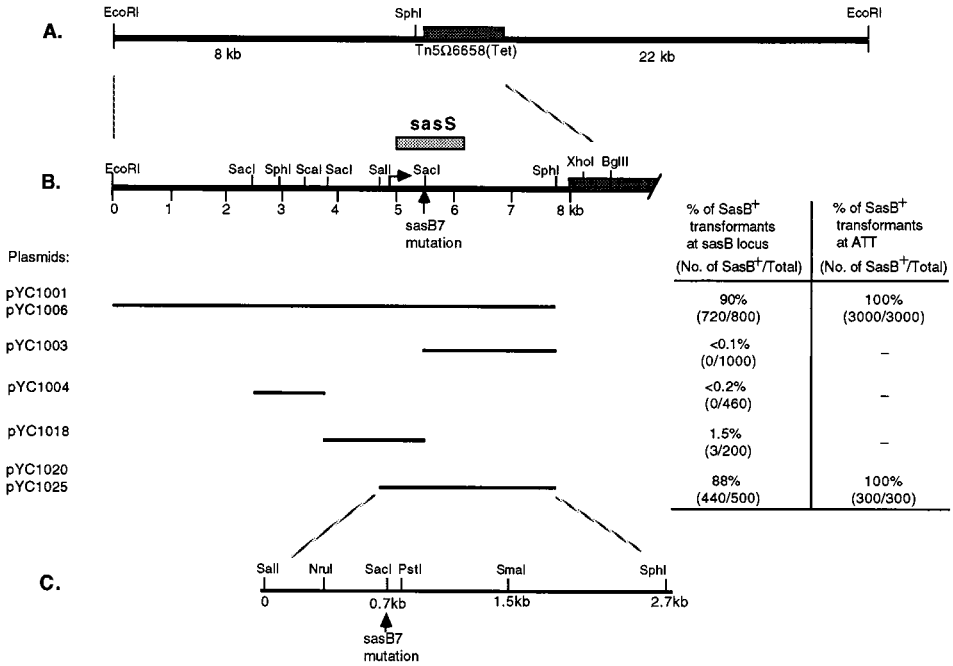

FIG. 1. Genetic analysis of the *sasB* locus. (A) Physical map of the *M. xanthus sasB* locus in strain DK6662 containing the linked Tn*5* Ω6658. The black line represents the *M. xanthus* DNA, and the dark shaded box represents Tn*5* DNA. (B) Restoration of the SasB$^+$ phenotype to the *sasB7* mutant DK6625 by wild-type *sasB* subclones integrated into the chromosomal *sasB* locus and the Mx8 phage attachment site, *attB*. The physical map of the *sasB* DNA cloned in pYC1001 is shown. The lightly shaded box represents the location of the *sasS* gene. The vertical arrow indicates the location of the *sasB7* mutation. The bent arrow indicates the direction of transcription and the location of the putative promoter. The dark shaded box indicates Tn*5* DNA. The bars beneath the physical map indicate the fragments present in the subclones. The percentage of SasB$^+$ transformants is calculated as the number of SasB$^+$ transformants divided by the total number of Km^r transformants tested, multiplied by 100. The SasB$^+$ colonies are tan on CTT agar overlaid with 0.04% X-Gal, and the SasB$^-$ colonies are blue under these conditions. The plasmids pYC1001, pYC1003, pYC1004, pYC1018, and pYC1020 were integrated as tandem duplications at the *sasB* locus. The plasmids pYC1006 and pYC1025 were integrated in *trans* at the *M. xanthus* Mx8 phage attachment site, *attB*. DK6625 (*sasB7 asgB480*) was the recipient strain. −, not tested. (C) Physical map of the *sasS*-containing subclone pYC1020.

indicate that this 8-kb fragment contains a functionally complete transcription unit. These data along with the results detailed above indicate that the wild-type allele is dominant to the *sasB7* allele when present in a heterozygotic merodiploid.

Mapping the *sasB7* mutation. To locate the position of the *sasB7* mutation within the 8-kb region, subclones of pYC1001 were constructed and introduced as tandem duplications into the *sasB7* mutant DK6625 to test their ability to restore the SasB$^+$ phenotype. In this case, only fragments carrying the wild-type version of the *sasB7* allele and at least one end of the functional transcription unit can restore the SasB$^+$ phenotype. When the cloned fragment contains the wild-type version of the *sasB7* allele and one truncated end of the transcription unit, a percentage of wild-type transformants arises from the total. This percentage indicates the relative distance between the mutation site and the truncated end of the transcription unit. The closer these elements are, the fewer wild-type transformants arise (16).

Plasmids pYC1003, pYC1004, pYC1018, and pYC1020 were electroporated into DK6625, creating tandem duplications at the chromosomal *sasB* locus. Electroporation of plasmid pYC1020 yielded 88% of the selected transformants with wild-type phenotypes (Fig. 1B). This percentage is close to that obtained with pYC1001 and is within the range of gene conversion events. These data suggest that pYC1020 carries the complete transcript unit.

To confirm that the fragment in plasmid pYC1020 contained the complete transcription unit and the wild-type version of the *sasB7* allele, the fragment in pYC1020 was introduced into the Mx8 phage attachment site in DK6625. Restoration of the wild-type phenotype was 100% (300 of 300), confirming that the 2.7-kb *Sal*I-*Sph*I fragment in pYC1020 contains the functionally complete transcription unit.

It is important to note that plasmid pYC1003, which contains the *Sph*I end present in pYC1020, did not restore the wild-type phenotype. This suggests that although it must contain one functional end, it does not contain the wild-type version of the *sasB7* allele. Plasmid pYC1018, which contains the *Sal*I end present in pYC1020, restored the wild-type phenotype at a very low frequency. This suggests that pYC1018 carries the wild-type version of the *sasB7* allele and that the mutation maps very close to its *Sac*I end. These data all place the site of the *sasB7* mutation very close to the *Sac*I restriction enzyme recognition site.

The *sasB7* allele maps to a gene encoding a histidine protein kinase. The nucleotide sequence of the 2.7-kb *Sal*I-*Sph*I fragment that contained the complete transcription unit and the wild-type version of the *sasB7* allele was determined. One ORF was predicted by the Genetics Computer Group Codonpreference program based on the G-C codon bias of the third position (2) in this high-G+C-content organism (41). Figure 2 shows the DNA and deduced amino acid sequence of the ORF and its surrounding region. The ORF is predicted to encode a 497-amino-acid protein of 52.6 kDa. It is predicted to start at nucleotide 218 and to stop at nucleotide 1711. No obvious ribosome-binding site has been observed upstream of the predicted translation start.

The ORF designated SasS is predicted to encode a histidine protein kinase, which is a member of the sensor protein family of the two-component signal transduction systems (21). The deduced amino acid sequence of SasS was subjected to the BLAST net search (1) of the databases. The SasS C-terminal

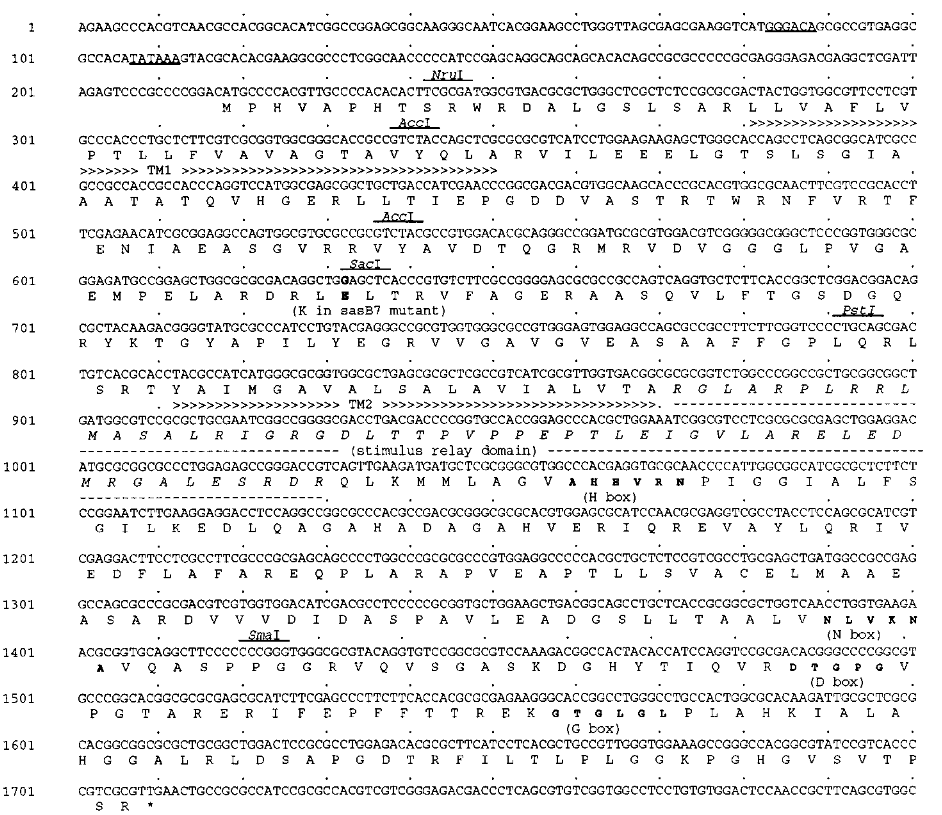

FIG. 2. DNA sequence and deduced amino acid sequence of *sasS* and its surrounding region. The DNA sequence, deduced amino acid sequence, and predicted functional domains of *sasS* are shown. The predicted start codon of SasS is at nucleotide 218. The predicted stop codon at nucleotide 1709 is marked by an asterisk. The putative −35 and −10 regions of the sigma70-like promoter are underlined. The *sasS* gene is predicted to encode a classical histidine protein kinase consisting of 497 amino acids (52.6 kDa). The two putative transmembrane domains are underlined with arrowheads. The conserved motifs (H, N, D, and G boxes) for histidine protein kinases are in boldface. The *sasB7* mutation is a G-to-A transition located within the predicted periplasmic region, which changes the E139 to K. The conserved stimulus relay domain is shown in italics and underlined with a dashed line.

kinase domain (amino acids 272 to 497) is about 26% identical to a group of histidine protein kinases (Fig. 3) (39, 42, 46, 60). The kinase domain of SasS contains a conserved N-terminal H box that contains the potential phosphorylation site, 282His. A similar histidine residue has been determined to be the phosphorylation site in the histidine protein kinase family (20, 44, 52). The SasS C-terminal kinase domain (amino acids 390 to 460) also contains the nucleotide binding regions, termed the N, D/F, and G boxes (45), that are highly conserved in all the histidine protein kinases (Fig. 2 and 3).

The SasS protein is predicted to be a transmembrane protein located in the cytoplasmic membrane. This argument is based principally on the primary sequence analysis of the N-terminal input domain. A hydrophobicity profile of SasS shows two hydrophobic regions, each of about 20 amino acids (amino acids 22 to 45 and 199 to 218), which flank a highly hydrophilic region (Fig. 2). The hydrophobic domains are each predicted to cross the cytoplasmic membrane, and the hydrophilic region is predicted to be a periplasmic domain. The two putative transmembrane domains were also identified by the TMpred program. BLAST searches showed that these two possible transmembrane domains are similar to TM1 and TM2 of the *E. coli* chemotaxis transducers (MCPs) (25 to 40 and 20 to 25% identity, respectively) (3, 5, 30). Interestingly, the whole N-terminal input domain (amino acids 1 to 190) of SasS has limited homology (about 21% identity) to all of the *E. coli* MCPs (3, 5, 30). In addition, a region of approximately 40 amino acids termed the "stimulus relay domain" (23), which is highly conserved in MCPs and other transmembrane sensor proteins, is also present in SasS. This domain is adjacent to the second transmembrane domain in all of the identified membrane sensors and has been shown to be important for signal transduction through the membrane (23). This region has not been observed in any cytoplasmic sensor proteins (23). Additional evidence to indicate the location and orientation of SasS comes from activity assays of SasS-PhoA fusion proteins (40). When analyzed in *E. coli* whole-cell lysates, the alkaline phosphatase activities of SasS-PhoA fusions were about four to seven times higher if they were fused to the predicted SasS periplasmic domain than if they were fused to the predicted cytoplasmic domain (data not shown).

The *sasB7* mutation is an E-to-K missense mutation at the N terminus of SasS. Mapping data (Fig. 1) indicated that the *sasB7* mutation was located close to the unique *Sac*I restriction enzyme recognition site within *sasS*. To identify the DNA alteration causing the *sasB7* mutant phenotype, the mutated *sasS* allele was cloned from DK6625 (*asgB480 sasB7*). An 850-bp *Sal*I-to-*Pst*I subclone (pYC1220) containing the *Sac*I site was sequenced. The *sasB7* mutation was found to be a G-to-A transition at nucleotide 632, which changes E139 to K. It was the only alteration in this DNA. Importantly, the mutation is located within the *Sac*I site and eliminates the site, thus confirming the mapping data. Furthermore, when this mutated DNA fragment was reintroduced into a wild-type strain, it recreated the SasB7 phenotype (62).

The *sasB7* mutation site is located on the hydrophilic side of

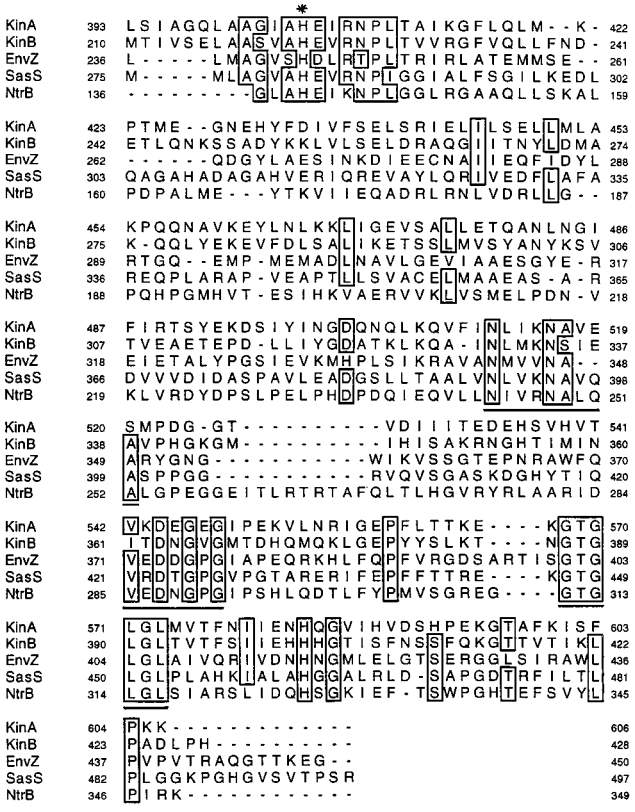

FIG. 3. Alignment of the deduced histidine protein kinase domain of SasS with the histidine protein kinase domains of KinA and KinB from *B. subtilis*, EnvZ from *E. coli*, and NtrB from *Klebsiella pneumoniae*. Each aligned sequence begins with an internal residue and ends with the C-terminal residue. The boxed amino acids are more than 80% identical among the aligned sequences (39, 42, 46, 60). The asterisk indicates the conserved histidine that has been determined to be the phosphorylation site in the family (20, 44, 52). The underlined sequences indicate the nucleotide binding domains (45).

a predicted amphiphilic α-helix (amino acids 122 to 142) within the periplasmic region of the SasS N-terminal input domain. This hydrophilic side is composed of six charged amino acids. In structures such as this, the charged face of the α-helix is the ligand interaction surface (64).

Null alleles of *sasS* abolish *4521* expression. Two *sasS* null strains were constructed to compare their effects on *4521* expression with the phenotype of the *sasB7* point mutation, which causes starvation- and A-signal-independent *4521* expression. One null strain, HK1503, which contains two mutated tandem copies of *sasS*, was generated by integrating a *sasS* internal fragment into the wild-type *sasS* gene. In this strain, one *sasS* gene is missing the 3′ end and the other is missing the 5′ end. The second null strain, HK1501, contains an omega kanamycin cassette (51) inserted into a unique *Nru*I site that is located at the predicted 10th codon of the *sasS* gene. This allele was generated by linearizing plasmid pYC1207 and introducing it into the wild-type strain, DK6620. The transformant HK1501, in which the wild-type *sasS* allele was replaced by the *sasS* null mutant allele, arose from a double crossover event.

The expression of *4521* in the *sasS* null mutants was dramatically different from that in the wild type and the *sasB7* mutant. Expression of *4521* remained at a basal level (5 to 10 U) during growth and development in both *sasS* null mutants. In contrast, *4521* expression in the wild type was about 10 U during growth and increased to almost 200 U during development, and *4521* expression in the *sasB7* mutant was about 540 U during growth and increased to more than 800 U during development (Fig. 4). The basal-level *4521* expression of the *sasS* null mutants indicates that SasS is a positive regulator of *4521*. This phenotype of the *sasS* null mutants was complemented when the wild-type *sasS* gene was placed in *trans* at the myxophage Mx8 attachment site, *attB*, indicating the null mutations do not interrupt a downstream gene (data not shown).

The high expression level of *4521* during growth and development in the *sasB7* mutant background indicates that this is a gain-of-function mutation. This expression data and the location of the mutation in the predicted periplasmic region of the N-terminal input domain suggest that the mutation alters the signaling state of the protein so that the kinase domain is constitutively phosphorylated.

SasS appears to function in response to extracellular A signal. Starvation and A signals activate *4521* expression in an *sasS*-dependent manner. To address the possibility that *sasS*-dependent *4521* expression results from *sasS* control of A-signal generation, the A-signal activity in supernatants of developing DK1622 (wild type) and HK1504 (*sasS* omega insertion null mutant) was measured. Supernatants from all of the strains had essentially the same level of extracellular A signal. The A-signal units measured in the supernatants of DK1622 and HK1504 were 2.9 and 9.6, respectively. These data indicate that the production of extracellular A signal is independent of *sasS*.

If SasS is involved in the response to A signal, then *sasS* null mutants should not respond to it. The response to A signal by *sasS* null mutants and wild-type cells was measured in low-density starving cells after the extracellular addition of various concentrations of the A-signal amino acid proline. Wild-type cells under these conditions phenotypically resemble the *asg* mutants, expressing low levels of *4521*, because at low density A signal does not surpass its critical-threshold concentration (36). When proline is added to wild-type cells within the 50 μM to 1 mM range, it provides A signal while maintaining the starvation conditions, and *4521* expression is rescued (Fig. 5). In contrast, no increase in *4521* expression was observed in the *sasS* null strain upon addition of proline. These data indicate

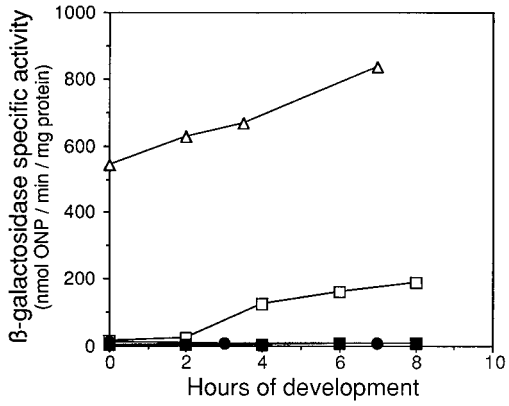

FIG. 4. Effects of *sasB* mutations on *4521* expression. β-Galactosidase specific activity of Tn*5 lac* Ω4521 in the wild-type strain DK6620 (□), the *sasB7* strain HK1412 (△), and the *sasS* null mutant strains HK1501 (■) and HK1503 (●) is shown. Cells containing Tn*5 lac* Ω4521 were harvested at different times during development on starvation agar. The specific β-galactosidase activity was determined as described in Materials and Methods. Each strain was tested in at least three independent experiments, and a representative experiment is shown. ONP, *o*-Nitrophenol.

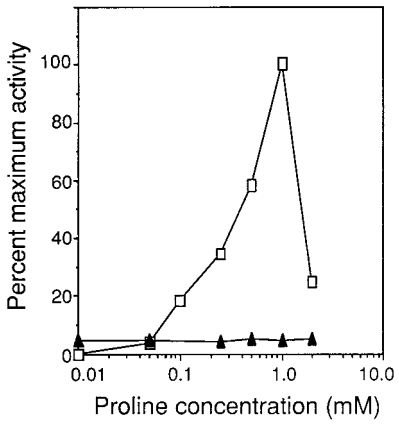

FIG. 5. Amino acid rescue of *4521* expression at low cell density. Different concentrations of proline were added to low-density wild-type DK6620 cells (□) and *sasS* null mutant HK1501 cells (▲). Percent maximum activity was calculated as the β-galactosidase activity divided by the peak level activity in wild-type cells. Each test was repeated at least twice, and a representative experiment is shown.

that the *sasS* null mutation blocks the A-signal response and that wild-type SasS functions in response to extracellular A signal.

Transcription of the *sasS* gene is constant during growth and development. If SasS functions as a sensor protein, it would be expected to be available for sensing during growth and development. However, it is formally possible that the *sasS*-dependent *4521* expression is a result of starvation and/or A-signal-stimulated transcription of *sasS*. To decide between these two possibilities, *sasS* transcription was monitored in the wild-type and *asgB480* backgrounds during growth and development. A promoterless *lacZ* gene was fused to the *sasS* gene, creating plasmid pYC1215. This plasmid was introduced into the *asgB480* mutant strain DK480 and transduced into the wild-type strain, DK101, creating strains HK1509 and HK1510, respectively. In both strains, a tandem duplication was present in which a wild-type *sasS* gene was separated from the *sasS-lacZ* transcriptional fusion by vector sequences. The β-galactosidase specific activity of HK1509 and HK1510 was measured during growth and development. A relatively low constant level of *sasS* expression was observed in the wild-type (11 to 15 U) and the *asgB480* (7 to 10 U) backgrounds during growth and development (Fig. 6). There was no evidence of any transcriptional regulation of *sasS*.

The *sasS* null mutants form defective fruiting bodies and exhibit reduced sporulation efficiency. To determine if SasS is involved in fruiting body development and/or sporulation, the *sasS* omega insertion null mutation was transferred into a wild-type background and these developmental characteristics were examined in submerged culture. The *sasS* null strain, HK1504, formed small abnormally shaped fruiting bodies that never appeared to mature or darken even after prolonged incubation. The sporulation analysis of the *sasS* null strain, HK1504, revealed a decreased sporulation efficiency. After 4 days of submerged culture development the *sasS* mutant formed 10% of the number of viable spores formed by the wild type. When these cell suspensions were allowed to develop for 7 days, the viable spore numbers of both the wild type and the *sasS* mutant decreased and the *sasS* mutant formed 5% of the number of viable spores formed by the wild type.

The observations that *sasS* mutants are deficient in fruiting body formation and sporulation demonstrate that SasS participates in *M. xanthus* development. However, the fact that 10% of the cells sporulated suggests that additional sensor kinases and/or other regulators are involved in the coordination of this complex developmental program. It is also possible that cross-talk among histidine kinases compensates for the absence of SasS.

DISCUSSION

The *sasS* gene encoding the first identified *M. xanthus* classic histidine protein kinase sensor that regulates early developmental gene expression was cloned and sequenced. The phenotypes of the *sasS* null mutants reveal that SasS functions as a key positive regulator of *4521* developmental expression, which is controlled independently by both starvation and cell density. As a classic histidine protein kinase sensor of the two-component signal transduction family, SasS has a C terminus which contains all of the conserved regions, including the phosphorylated histidine and its surrounding H box and the nucleotide binding N, D/F, and G boxes. The N terminus of SasS is predicted to contain two transmembrane regions that would place the protein in the cytoplasmic membrane. SasS most likely controls the developmental expression of *4521* and other genes in this class by regulating phosphate transfer to its cognate response regulator.

SasS appears to be an essential component of the transduction pathway that regulates *4521* developmental expression in response to environmental changes. First, the *sasS* null mutant produces A signal at wild-type levels, indicating that SasS is not involved in the generation of A signal. Second, as would be expected of strains lacking a transducer, the *sasS* null mutants do not respond to exogenous A signal (Fig. 5). Third, the *sasS* gene encoding the sensor is not regulated at the level of transcription (Fig. 6), suggesting that the protein monitors environmental changes during growth and development.

It is possible that starvation and A signals are integrated through cooperative control of SasS phosphorylation. The data supporting this idea come from *4521* expression levels in different *sasS* mutants. First, the *4521* gene is expressed at a basal level in the *sasS* null mutants even when the cells are starved and A signal is present (Fig. 4). Second, the gain-of-function

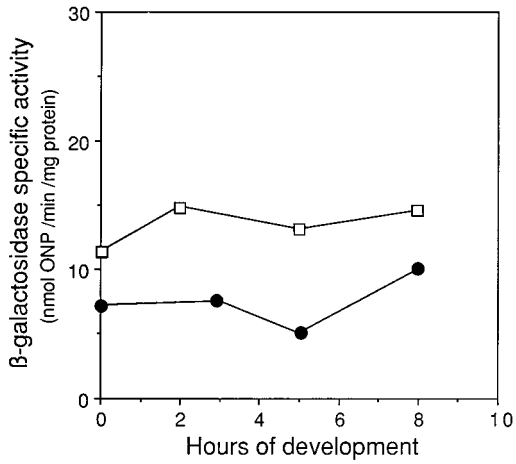

FIG. 6. Expression of *sasS-lacZ* during growth and development in wild-type and *asgB* backgrounds. Strain HK1510 (□) carries a *sasS-lacZ* transcriptional fusion in a wild-type background. Strain HK1509 (●) carries a *sasS-lacZ* transcriptional fusion in the *asgB480* background. Both strains contain the *sasS-lacZ* fusion in addition to a wild-type *sasS* gene. β-Galactosidase specific activity was analyzed in growing and developing cells as described in Materials and Methods. Each strain was tested in at least three independent experiments, and a representative experiment is shown. ONP, *o*-Nitrophenol.

sasS mutation, *sasB7*, bypasses the starvation and A-signal requirements, allowing *4521* expression during growth and in the absence of A signal (Fig. 4).

The SasB7 gain-of-function phenotype most likely results in inappropriate phosphate transfer to the downstream cognate response regulator. The location of the *sasB7* mutation in the putative periplasmic region of the N-terminal input domain suggests that this mutation indirectly influences the activity of the C-terminal kinase domain. This could be done through stimulation of autokinase activity or inactivation of an intrinsic phosphatase activity. One unusual feature of the *sasB7* gain-of-function mutant allele is that it is recessive to the wild type when present as a heterozygotic merodiploid (Fig. 1). The most likely explanation is that SasS functions as an oligomer and that for a SasB7 phenotype all or most of the subunits must be mutants. Another unusual feature of the *sasB7* gain-of-function mutation is that it does not confer an obvious vegetative or developmental phenotype on an otherwise wild-type strain. This suggests that *M. xanthus* cells can compensate for the inappropriate stimulation of this signal transduction pathway.

If SasS integrates starvation and A-signal information, the SasS phosphorylation level should respond to the cells' nutrient status and density. It should transduce this information by controlling the threshold level of phosphate transfer to its cognate response regulator. In this case, SasS would serve as a checkpoint, blocking development if conditions are not appropriate. Integration of starvation and A signals does not require that both signals be directly sensed by SasS. It is possible that the A signal is sensed directly and starvation modulates the ability of the kinase domain to be activated, so that it is only phosphorylated during starvation.

It is also possible that starvation or A-signal control of *4521* expression is transduced through another input. Either of these conditions could influence the activity of another positive regulatory element, such as a histidine kinase sensor, a response regulator, or another type of activator. In this case, the input would be considered accessory. This input alone is not adequate to stimulate the response regulator, because there is only basal *4521* expression in the *sasS* null mutant in the presence of either starvation or A signal (Fig. 4).

How is A signal sensed? SasS could directly sense A signal by determining if the periplasmic amino acid concentration is above the 10 μM threshold. This type of mechanism would be typical of the interactions between a ligand and its binding protein. This possibility is particularly interesting when it is considered that A signal is a set of amino acids and that the predicted SasS N-terminal input domain structure is similar to that of the MCP chemoreceptors, many of which directly sense amino acids. In addition, it should be noted that the minimum threshold A-signal concentration of 10 μM for any given A-signal amino acid is in the range of the minimum amino acid concentration (10^{-5} to 10^{-7} M) necessary for a Tsr-mediated chemotactic response in *E. coli* (19).

How is starvation integrated? One way in which starvation could be integrated is by resetting the sensitivity of SasS to amino acids. If SasS senses A signal as an amino acid level greater than 10 μM, it is surprising that it is not activated by the high extracellular concentrations of amino acids during growth. Considering the adaptation response of the chemoreceptors (23, 59), it is possible that during growth SasS is modified and desensitized to the high amino acid concentration. Starvation could function to inactivate this modification, allowing for SasS phosphorylation when the A-signal amino acids surpass the 10 μM threshold. One likely candidate to control adaptation of SasS is the negative regulator, SasB5, that maps downstream of *sasS* and appears from epistasis experiments (61) to function upstream of SasS.

What functions downstream of SasS? It is likely that the cognate response regulator of SasS would be an NtrC-like homolog that could directly activate transcription of the *4521* sigma54-dependent promoter. Interestingly, we have genetically identified an NtrC-like response regulator that maps 2.2 kb downstream of *sasS*. Mutational analysis of this gene indicates that the response regulator is a positive regulator of *4521* expression. In addition, epistasis experiments indicate that the response regulator functions downstream of SasS and suggest they may be a cognate pair (62). This response regulator is among the 14 NtrC-like response regulators recently identified by amplification of *M. xanthus* chromosomal DNA by PCR (28). It is likely that SasS regulates genes other than *4521*, especially since an insertion mutation in the *4521* gene does not seem to affect *M. xanthus* development (14). To identify additional targets regulated by the SasS sensor kinase, we are currently testing a variety of other *lacZ* transcriptional fusions expressed during early *M. xanthus* development.

The data presented here indicate that the SasS sensor kinase is the major regulator of *4521* expression, because the *sasS* null mutations essentially abolish *4521* developmental expression. Thus, the simplest model for control of *4521* expression is one in which starvation and cell density inputs feed into one sensor kinase, SasS, that activates one response regulator. However, the regulation of multicellular development appears to be more complex, because the *sasS* null mutations do not severely block development. Recent data suggest that a variety of inputs, including cell surface properties (16) and directed cell movement (63), in addition to starvation and cell density, contribute to the initiation of *M. xanthus* development. It is possible that SasS is one member of a phosphorelay system that integrates these inputs. This *M. xanthus* phosphorelay system could resemble that utilized by *Bacillus subtilis* to initiate sporulation (47, 56). Another intriguing possibility is that a branched network of regulators coordinates the complex behavioral response of *M. xanthus* fruiting body development.

ACKNOWLEDGMENTS

We thank W. Margolin and J. Eraso for comments on the manuscript.

This investigation was supported by Public Health Service grant GM47444 to H.B.K. from the National Institutes of Health.

REFERENCES

1. **Altschul, S. F., W. Gish, W. Miller, E. W. Myers, and D. J. Lipman.** 1990. Basic local alignment search tool. J. Mol. Biol. **215:**403–410.
2. **Bibb, M. J., P. R. Findlay, and M. W. Johnson.** 1984. The relationship between base composition and codon usage in bacterial genes and its use for the simple and reliable identification of protein-coding sequences. Gene **30:**157–166.
3. **Bollinger, J., C. Park, S. Harayama, and G. L. Hazelbauer.** 1984. Structure of the Trg protein: homologies with and differences from other sensory transducers of *Escherichia coli*. Proc. Natl. Acad. Sci. USA **81:**3287–3291.
4. **Bowden, M. G., and H. B. Kaplan.** 1996. The *Myxococcus xanthus* developmentally expressed *asgB*-dependent genes can be targets of the A signal-generating or A signal-responding pathway. J. Bacteriol. **178:**6628–6631.
5. **Boyd, A., K. Kendall, and M. I. Simon.** 1983. Structure of the serine chemoreceptor in *Escherichia coli*. Nature **301:**623–626.
6. **Bradford, M. M.** 1976. A rapid and sensitive method for the quantitation of microgram quantities of protein utilizing the principle of protein-dye binding. Anal. Biochem. **72:**248–254.
7. **Campos, J. M., J. Geisselsoder, and D. R. Zusman.** 1978. Isolation of bacteriophage MX4, a generalized transducing phage for *Myxococcus xanthus*. J. Mol. Biol. **119:**167–178.
8. **Davis, J. M., J. Mayor, and L. Plamann.** 1995. A missense mutation in *rpoD* results in an A signaling defect in *Myxococcus xanthus*. Mol. Microbiol. **18:**943–952.
9. **Devereux, J., P. Haeberli, and O. Smithies.** 1984. A comprehensive set of sequence analysis programs for the VAX. Nucleic Acids Res. **12:**387–395.

10. **Dworkin, M.** 1996. Recent advances in the social and developmental biology of the myxobacteria. Microbiol. Rev. **60:**70–102.
11. **Dworkin, M., and D. Kaiser.** 1993. Myxobacteria II. American Society for Microbiology, Washington, D.C.
12. **Geisselsoder, J., J. M. Campos, and D. R. Zusman.** 1978. Physical characterization of bacteriophage MX4, a generalized transducing phage for *Myxococcus xanthus*. J. Mol. Biol. **119:**179–189.
13. **Gill, R. E., M. G. Cull, and S. Fly.** 1988. Genetic identification and cloning of a gene required for developmental cell interactions in *Myxococcus xanthus*. J. Bacteriol. **170:**5279–5288.
14. **Gulati, P., J. Gibson, and H. B. Kaplan.** Unpublished data.
15. **Gulati, P., D. Xu, and H. B. Kaplan.** 1995. Identification of the minimum regulatory region of a *Myxococcus xanthus* A-signal-dependent developmental gene. J. Bacteriol. **177:**4645–4651.
16. **Guo, D., M. G. Bowden, R. Pershad, and H. B. Kaplan.** 1996. The *Myxococcus xanthus rfbABC* operon encodes an ABC transporter homolog required for O-antigen biosynthesis and multicellular development. J. Bacteriol. **178:** 1631–1639.
17. **Hagen, D. C., A. P. Bretscher, and D. Kaiser.** 1978. Synergism between morphogenetic mutants of *Myxococcus xanthus*. Dev. Biol. **64:**284–296.
18. **Hanahan, D.** 1983. Studies on transformation of *Escherichia coli* with plasmids. J. Mol. Biol. **166:**557–580.
19. **Hedblom, M., and J. Adler.** 1983. Chemotactic response of *Escherichia coli* to chemically synthesized amino acids. J. Bacteriol. **155:**1463–1466.
20. **Hess, J. F., R. B. Bourret, and M. Simon.** 1988. Histidine phosphorylation and phosphoryl group transfer in bacterial chemotaxis. Nature **336:**139–143.
21. **Hoch, J. A., and T. J. Silhavy.** 1995. Two-component signal transduction. American Society for Microbiology, Washington, D.C.
22. **Hodgkin, J., and D. Kaiser.** 1977. Cell-to-cell stimulation of movement in nonmotile mutants of *Myxococcus*. Proc. Natl. Acad. Sci. USA **74:**2938–2942.
23. **Hoff, W. D., K.-H. Jung, and J. L. Spudich.** 1997. Molecular mechanism of photosignaling by archeal sensory rhodopsins. Annu. Rev. Biophys. Biomol. Struct. **26:**221–256.
24. **Kaiser, D.** 1979. Social gliding is correlated with the presence of pili in *Myxococcus xanthus*. Proc. Natl. Acad. Sci. USA **76:**5952–5956.
25. **Kaplan, H. B., A. Kuspa, and D. Kaiser.** 1991. Suppressors that permit A-signal-independent developmental gene expression in *Myxococcus xanthus*. J. Bacteriol. **173:**1460–1470.
26. **Kaplan, H. B., and L. Plamann.** 1996. A *Myxococcus xanthus* cell density-sensing system required for multicellular development. FEMS Microbiol. Lett. **139:**89–95.
27. **Kashefi, K., and P. L. Hartzell.** 1995. Genetic suppression and phenotypic masking of a *Myxococcus xanthus frzF*$^-$ defect. Mol. Microbiol. **15:**483–494.
28. **Kaufman, R. I., and B. T. Nixon.** 1996. Use of PCR to isolate genes encoding σ^{54}-dependent activators from diverse bacteria. J. Bacteriol. **178:**3967–3970.
29. **Keseler, I. M., and D. Kaiser.** 1995. An early A-signal-dependent gene in *Myxococcus xanthus* has a σ^{54}-like promoter. J. Bacteriol. **177:**4638–4644.
30. **Krikos, A., N. Mutoh, A. Boyd, and M. I. Simon.** 1983. Sensory transducers of *E. coli* are composed of discrete structural and functional domains. Cell **33:**615–622.
31. **Kroos, L., A. Kuspa, and D. Kaiser.** 1986. A global analysis of developmentally regulated genes in *Myxococcus xanthus*. Dev. Biol. **117:**252–266.
32. **Kuner, J. M., and D. Kaiser.** 1982. Fruiting body morphogenesis in submerged cultures of *Myxococcus xanthus*. J. Bacteriol. **151:**458–461.
33. **Kuspa, A., and D. Kaiser.** 1989. Genes required for developmental signalling in *Myxococcus xanthus*: three *asg* loci. J. Bacteriol. **171:**2762–2772.
34. **Kuspa, A., L. Kroos, and D. Kaiser.** 1986. Intercellular signaling is required for developmental gene expression in *Myxococcus xanthus*. Dev. Biol. **117:** 267–276.
35. **Kuspa, A., L. Plamann, and D. Kaiser.** 1992. Identification of heat-stable A-factor from *Myxococcus xanthus*. J. Bacteriol. **174:**3319–3326.
36. **Kuspa, A., L. Plamann, and D. Kaiser.** 1992. A-signalling and the cell density requirement for *Myxococcus xanthus* development. J. Bacteriol. **174:**7360–7369.
37. **Kustu, S., E. Santero, J. Keener, D. Popham, and D. Weiss.** 1989. Expression of σ^{54} (*ntrA*)-dependent genes is probably united by a common mechanism. Microbiol. Rev. **53:**367–376.
38. **LaRossa, R., J. Kuner, D. Hagen, C. Manoil, and D. Kaiser.** 1983. Developmental cell interactions of *Myxococcus xanthus*: analysis of mutants. J. Bacteriol. **153:**1394–1404.
39. **Macfarlane, S. A., and M. Merrick.** 1985. The nucleotide sequence of the nitrogen regulation gene *ntrB* and the *glnA-ntrBC* intergenic region of *Klebsiella pneumoniae*. Nucleic Acids Res. **13:**7591–7606.
40. **Manoil, C., and J. Beckwith.** 1985. Tn*phoA*: a transposon probe for protein export signals. Proc. Natl. Acad. Sci. USA **82:**8129–8133.
41. **Mesbah, M., U. Premachandran, and W. B. Whitman.** 1989. Precise measurement of the G+C content of deoxyribonucleic acid by high-performance liquid chromatography. Int. J. Syst. Bacteriol. **39:**159–167.
42. **Mizuno, T., E. T. Wurtzel, and M. Inouye.** 1982. Osmoregulation of gene expression. II. DNA sequence of the *envZ* gene of the *ompB* operon of *Escherichia coli* and characterization of its gene product. J. Biol. Chem. **257:**13692–13698.
43. **Morett, E., and L. Segovia.** 1993. The σ^{54} bacterial enhancer-binding protein family: mechanism of action and phylogenetic relationship of their functional domains. J. Bacteriol. **175:**6067–6074.
44. **Ninfa, A. J., and R. L. Bennett.** 1991. Identification of the site of autophosphorylation of the bacterial protein kinase/phosphatase NRII. J. Biol. Chem. **266:**6888–6893.
45. **Parkinson, J. S., and E. C. Kofoid.** 1992. Communication modules in bacterial signaling proteins. Annu. Rev. Genet. **26:**71–112.
46. **Perego, M., S. P. Cole, D. Burbulys, K. Trach, and J. A. Hoch.** 1989. Characterization of the gene for a protein kinase which phosphorylates the sporulation-regulatory proteins Spo0A and Spo0F of *Bacillus subtilis*. J. Bacteriol. **171:**6187–6196.
47. **Perego, M., P. Glaser, and J. Hoch.** 1996. Aspartyl-phosphate phosphatases deactivate the response regulator components of the sporulation signal transduction system in *Bacillus subtilis*. Mol. Microbiol. **19:**1151–1157.
48. **Plamann, L., J. M. Davis, B. Cantwell, and J. Mayor.** 1994. Evidence that *asgB* encodes a DNA-binding protein essential for growth and development of *Myxococcus xanthus*. J. Bacteriol. **176:**2013–2020.
49. **Plamann, L., A. Kuspa, and D. Kaiser.** 1992. Proteins that rescue A-signal-defective mutants of *Myxococcus xanthus*. J. Bacteriol. **174:**3311–3318.
50. **Plamann, L., Y. Li, B. Cantwell, and J. Mayor.** 1995. The *Myxococcus xanthus asgA* gene encodes a novel signal transduction protein required for multicellular development. J. Bacteriol. **177:**2014–2020.
51. **Prentki, P., and H. M. Krisch.** 1984. *In vivo* insertional mutagenesis with a selectable DNA fragment. Gene **29:**303–313.
52. **Roberts, D. L., D. W. Bennett, and S. A. Forst.** 1993. Identification of the site of phosphorylation on the osmosensor, EnvZ, of *Escherichia coli*. J. Biol. Chem. **269:**8728–8733.
53. **Sambrook, J., E. F. Fritsch, and T. Maniatis.** 1989. Molecular cloning: a laboratory manual, 2nd ed. Cold Spring Harbor Laboratory Press, Cold Spring Harbor, N.Y.
54. **Shimkets, L. J., R. E. Gill, and D. Kaiser.** 1983. Developmental cell interactions in *Myxococcus xanthus* and the *spoC* locus. Proc. Natl. Acad. Sci. USA **80:**1406–1410.
55. **Singer, M., and D. Kaiser.** 1995. Ectopic production of guanosine penta- and tetraphosphate can initiate early developmental gene expression in *Myxococcus xanthus*. Genes Dev. **9:**1633–1644.
56. **Solomon, J., B. Lazazzera, and A. Grossman.** 1996. Purification and characterization of an extracellular peptide factor that affects two different developmental pathways in *Bacillus subtilis*. Genes Dev. **10:**2014–2024.
57. **Spratt, B. G., P. J. Hedge, S. Heesen, A. Edelman, and J. K. Broome-Smith.** 1986. Kanamycin-resistant vectors that are analogues of plasmids pUC8, pUC9, pEMBL8, and pEMBL9. Gene **41:**337–342.
58. **Stephens, K., and D. Kaiser.** 1987. Genetics of gliding motility in *Myxococcus xanthus*: molecular cloning of the *mgl* locus. Mol. Gen. Genet. **207:**256–266.
59. **Stock, J. B., and M. G. Surette.** 1996. Chemotaxis, p. 1103–1120. *In* F. C. Neidhardt, R. Curtiss III, J. L. Ingraham, E. C. C. Lin, K. B. Low, B. Magasanik, W. S. Reznikoff, M. Riley, M. Schaechter, and H. E. Umbarger (ed.), *Escherichia coli* and *Salmonella*: cellular and molecular biology, 2nd ed. American Society for Microbiology, Washington, D.C.
60. **Trach, K. A., and J. A. Hoch.** 1993. Multisensory activation of the phosphorelay initiating sporulation in *Bacillus subtilis*: identification and sequence of the protein kinase of the alternate pathway. Mol. Microbiol. **8:**69–79.
61. **Xu, D., C. Yang, and H. B. Kaplan.** Unpublished data.
62. **Yang, C., and H. B. Kaplan.** Unpublished data.
63. **Yang, Z., D. Xu, Y. Geng, H. B. Kaplan, and W. Shi.** Unpublished data.
64. **Zhu, Z.-Y., and S. Karlin.** 1996. Clusters of charged residues in protein three-dimensional structures. Proc. Natl. Acad. Sci. USA **193:**8350–8355.